ELSEVIER

Journal of Quantitative Spectroscopy & Radiative Transfer 103 (2007) 394–401

Journal of Quantitative Spectroscopy & Radiative Transfer

www.elsevier.com/locate/jqsrt

Electromagnetic energy flow near metal nanoparticles—II: Algorithms for the calculation of the light scattering of multi-spheres and photon energy transport via linear chains of Ag nanoparticles

Zhipeng Li[a], Hongxing Xu[a,b,*]

[a]*Institute of Physics, Chinese Academy of Science, Beijing 100080, China*
[b]*Division of Solid State Physics, Lund University, Box 118, S-22100, Sweden*

Received 1 June 2006; received in revised form 19 June 2006; accepted 20 June 2006

Abstract

We present a new algorithm to calculate the near-field distribution of scattered light of multiple nanospheres based on recursive order-of-scattering (OS) and the matrix inversion approaches, which avoids the divergent problem encountered in origin OS method at the resonance condition. Using this method, we investigate the light-transport properties of linear chains of Ag nanospheres. We found a maximum 3 dB damping length of 1.4 μm of the light propagation when the first sphere of the linear Ag spheres with the radius $R = 25$ nm was illuminated. The optimal configurations that favor the photon energy transport are investigated as well.

Keywords: Mie theory; Multi-sphere; Ag nanoparticles

1. Introduction

In a recent paper [1], we studied the electromagnetic energy flow near a single sphere (referred as part I). In this paper, we will focus on the case of multi-spheres. We will firstly develop a recursive algorithm for the light scattering of multi-spheres. Then we will investigate the electromagnetic energy transport via linear chains of Ag nanospheres. For multi-spheres, the electromagnetic near-field distribution has attracted increasing interests recently [2–4]. The analytical solution of the light scattering of aggregates can be obtained by extending Mie theory [5–7]. In the Mie theory [8], the scattering of light by a single sphere situated in a homogeneous medium was solved directly as a boundary condition problem. More complex scattering problems of aggregates [5–7,9–15] need to be solved by the generalized Mie theory, which uses either T-matrix method [9,10] or the order-of-scattering (OS) method [6,7]. The generalized Mie theory is widely used in the calculation of near-field optics, such as single-molecule surface-enhanced Raman scattering [16,17] and

*Corresponding author. Institute of Physics, Chinese Academy of Science, Beijing 100080, China.
E-mail address: hongxingxu@aphy.iphy.ac.cn (H. Xu).

0022-4073/$ - see front matter © 2006 Elsevier Ltd. All rights reserved.
doi:10.1016/j.jqsrt.2006.06.007

integrated optics [2,4]. Although a lot of other calculation methods such as discrete dipole approximation [18], and the finite-difference time-domain [19] have been also well developed, the generalized Mie theory is more rigorous and powerful for spherical nanoparticles as its lower computational demand than other methods [5,20,21].

Based on the Mie theory, the T-matrix approach which was introduced by Waterman [22] is widely used. Similar to the original Mie theory, the incident and scattered field are expanded into the vector spherical harmonics (VSH), where the addition theorem for translations of VSH translating between coordinates originated at the centers of different spheres is applied [23]. The scattered field can be obtained directly by solving linear system of equations which contain Mie scattering coefficients and the translation coefficients [7]. Various techniques to calculate T-matrix of multi-spheres have been reported, such as iterative [24] and recursive [25] method. However, this method is tedious when the distances between spheres turn to small or the number of spheres L becomes large. As the decreasing of distance between spheres, multi-polars of higher order have to be considered, that increases the size of equations, while the increasing of the number of spheres L naturally increases the size of equations. Another approach used in the generalized Mie theory is the OS method in which the field of scattered light is expressed as a sum of scattered field of different orders. By tracing the light path between spheres, scattered field in each scattering event can be obtained by applying boundary conditions of single sphere. The solution of two spheres was given by Fuller [7]. Recently, we developed an recursive OS algorithm to calculate the near-field distribution of the scattered field of multiple nanospheres [26]. The OS method is usually fast than T-matrix approaches in many cases, when a fast convergence happens for rather small OS [7]. However, it is not the case at the resonance, where the convergence cannot be obtained even for very high OS [20,27]. One way to avoid this divergent problem is substituting the summation of different OS by matrix inversion (MI). Such an approach is known for the case of two spheres [6], but the complex scattering events for multi-spheres still need more careful consideration in order to obtain a proper expression.

Here we develop a proper MI approach based on the recursive OS method for multiple nanospheres, which can avoid the divergent problem at resonance conditions. The advantage is also that the dimension of matrix for inversion carried in our method is still same as a single particle, which results L^2 times smaller than the T-matrix approach; hence our algorithm consumes less computational time.

This newly developed MI method is then applied to investigate the light-transport properties of linear chains of Ag nanospheres, which has recently become an interesting subfield of plasmon-assisted waveguide [2]. Different from Quinten et al. [4] where a linear chain of Ag nanoparticles was investigated at a fixed resonant frequency of an isolated Ag sphere, we will investigate the interested frequency range to find the optimal transport conditions. Due to the coupling between Ag spheres in the chain, the resonant frequency of chain can be largely different from the isolated sphere and this resonant frequency varies with the width of the gap between two adjacent spheres. A certain incident frequency will correspond to a most favorite geometry, and vice versa.

2. Method

Based on the Mie theory [8], both the incident electric field and the scattered electric field of the ensemble of L spheres can be expanded in the form of the VSH as:

$$\begin{aligned} {}^{\mathrm{i}}E_l &= \sum_{n=1}^{\infty}\sum_{m=-n}^{n}\sum_{p=1}^{2} {}^{\mathrm{i}}C_{mnp}^{l}\left|mn1p\right\rangle, \\ {}^{\mathrm{s}}E = \sum_{l=1}^{\oplus L} {}^{\mathrm{s}}\mathrm{E}_l &= \sum_{l=1}^{\oplus L}\sum_{n=1}^{\infty}\sum_{m=-n}^{n}\sum_{p=1}^{2} {}^{\mathrm{s}}C_{mnp}^{l}\left|mn3p\right\rangle, \end{aligned} \tag{1}$$

where ${}^{\mathrm{i}}C_{mnp}^{l}$ and ${}^{\mathrm{s}}C_{mnp}^{l}$ are the expansion coefficients for the VHS $\left|mnjp\right\rangle$ centered at the lth sphere, with $p=1$ for $\mathbf{M}_{mn}^{j}$ and $p=2$ for $\mathbf{N}_{mn}^{j}$, respectively, n is the number of multi-poles and m is the corresponding angular number, and $j=1, 2, 3, 4$ corresponds to spherical functions j_n, y_n, $h_n^{(1)}$, respectively [28]. The symbol $\oplus$ means that the sum should occur in Cartesian coordinates. By summing single scattering events, the scattering coefficients ${}^{\mathrm{s}}C_{mnp}^{l}$ are functions of the incident coefficients ${}^{\mathrm{i}}C_{mnp}^{l}$, the corresponding Lorenz–Mie coefficients a_n^l

and b_n^l, and the translation coefficients ${}^{lh}A_{mn}^{\mu\nu}$ and ${}^{lh}B_{mn}^{\mu\nu}$ between sphere l and sphere h [29,30], and written as:

$$ {}^{s}C_{mnp}^{l} = {}^{L}T_l({}^{i}C_{\mu\nu q}^{h}, a_v^h, b_v^h, {}^{lh}A_{mn}^{\mu\nu}, {}^{lh}B_{mn}^{\mu\nu}). \tag{2} $$

The corresponding magnetic fields are expanded as:

$$ \begin{aligned} {}^{i}H_l &= \tfrac{k}{i\omega\mu}\sum_{n=1}^{\infty}\sum_{m=-n}^{n}\sum_{p=1\neq p'}^{2} {}^{i}C_{mnp}^{l}\left|mn1p'\right\rangle, \\ {}^{s}H = \tfrac{k}{i\omega\mu}\sum_{l=1}^{\oplus L}{}^{s}H_l &= \tfrac{k}{i\omega\mu}\sum_{l=1}^{\oplus L}\sum_{n=1}^{\infty}\sum_{m=-n}^{n}\sum_{p=1\neq p'}^{2} {}^{s}C_{mnp}^{l}\left|mn3p'\right\rangle, \end{aligned} \tag{3} $$

due to the simple relation between the **E** field and the **H** field, and the relations between the normal modes: $\mathbf{H} = 1/i\omega\mu\nabla\mathbf{E}$, $\mathbf{N} = 1/k\nabla\mathbf{M}$, $\mathbf{M} = 1/k\nabla\mathbf{N}$.

In order to calculate Eq. (2), we define the matrix representation of the scattering matrix T as the function of the matrix G of the incident coefficients [26] and the response matrix Ψ of the L-spheres system. For a single sphere, the scattering matrix is simply written as:

$$ {}^{1}T = G_1\Psi^{(1)}, \tag{4} $$

where $\Psi^{(1)} = S_1$, and S_1 is the matrix of the Mie scattering coefficients of this single particle as defined in Ref. [26].

Similar to Ref. [26], the scattering matrixes of two spheres are:

$$ \begin{aligned} {}^{2}T_1 &= (G_1S_1 + G_2S_2\Omega_{21}S_1)\sum_{i=0}^{Nos}(\Omega_{12}S_2\Omega_{21}S_1)^i, \\ {}^{2}T_2 &= (G_2S_2 + G_1S_1\Omega_{12}S_2)\sum_{i=0}^{Nos}(\Omega_{21}S_1\Omega_{12}S_2)^i. \end{aligned} \tag{5} $$

In order to use the response matrix, Eq. (5) is rewritten as:

$$ \left({}^{2}T_1, {}^{2}T_2\right) = (G_1, G_2)\Psi^{(2)}, \tag{6} $$

where

$$ \Psi^{(2)} = \begin{pmatrix} S_1\sum_{i=0}^{Nos}(\Omega_{12}S_2\Omega_{21}S_1)^i & S_1\Omega_{12}S_2\sum_{i=0}^{Nos}(\Omega_{21}S_1\Omega_{12}S_2)^i \\ S_2\Omega_{21}S_1\sum_{i=0}^{Nos}(\Omega_{12}S_2\Omega_{21}S_1)^i & S_2\sum_{i=0}^{Nos}(\Omega_{21}S_1\Omega_{12}S_2)^i \end{pmatrix}. $$

The summation of scattering orders here can be accounted for to the infinite order by the matrix inverse:

$$ \sum_{i=0}^{Nos}(\Omega_{kj}S_j\Omega_{jk}S_k)^i = \frac{1}{1-\Omega_{kj}S_j\Omega_{jk}S_k}. \tag{7} $$

When the third sphere is added, this new sphere is irradiated by both the incident light and scattering light from 1 and 2 spheres, and scattered back and forth. The scattering matrix of the added sphere is

$$ {}^{3}T_3 = ((G_1, G_2)\Psi^{(2)}\Omega'^{(2)}S_3 + G_3S_3)\sum_{i=0}^{Nos}\left(\Omega^{(2)}\Psi^{(2)}\Omega'^{(2)}S_3\right)^i, \tag{8} $$

where

$$ \Omega^{(2)} = \left(\Omega_{3,1}, \Omega_{3,2}\right), \quad \Omega'^{(2)} = \begin{pmatrix} \Omega_{1,3} \\ \Omega_{2,3} \end{pmatrix}. $$

In the format of the response matrix, Eq. (8) is rewritten as:

$$ {}^3T_3 = (G_1, G_2, G_3)\begin{pmatrix} \Psi_{13}^{(3)} \\ \Psi_{23}^{(3)} \\ \Psi_{33}^{(3)} \end{pmatrix}, \tag{9} $$

where

$$ \Psi_{33}^{(3)} = S_3 \sum_{i=0}^{Nos} (\Omega^{(2)}\Psi^{(2)}\Omega'^{(2)}S_3)^i, $$

$$ \Psi_{i3}^{(3)} = \sum_{j=1}^{2} \Psi_{ij}^{(2)}\Omega_{j,3}\Psi_{33}^{(3)} \quad i = 1, 2. $$

For 1st and 2nd sphere again, both the scattered light from 3rd sphere and the incident light work as the illumination field. With the known scattering matrix of the 3rd sphere, similar to Eq. (5), the scattering matrixes of 1 and 2 spheres are:

$$ ({}^3T_1, {}^3T_2) = [(G_1, G_2) + {}^3T_3\Omega^{(2)}]\Psi^{(2)}. \tag{10} $$

In the format of the response matrixes and by inserting Eq. (9), it is not difficult to obtain:

$$ \left({}^3T_1, {}^3T_2\right) = (G_1, G_2, G_3)\begin{pmatrix} \Psi_{11}^{(3)} & \Psi_{12}^{(3)} \\ \Psi_{21}^{(3)} & \Psi_{22}^{(3)} \\ \Psi_{31}^{(3)} & \Psi_{32}^{(3)} \end{pmatrix}, \tag{11} $$

where

$$ \Psi_{ij}^{(3)} = \Psi_{ij}^{(2)} + \Psi_{i3}^{(3)} \sum_{k=1}^{2} \Omega_{3,k}\Psi_{kj}^{(2)} \quad i,j = 1, 2 $$

$$ \Psi_{3i}^{(3)} = \Psi_{33}^{(3)} \sum_{k=1}^{2} \Omega_{3,k}\Psi_{ki}^{(2)} \quad i = 1, 2. $$

Combining with Eq. (9) and Eq. (11), the scattering matrixes of 3-sphere system can be obtained:

$$ \left({}^3T_1, {}^3T_2, {}^3T_3\right) = (G_1, G_2, G_3)\Psi^{(3)}. \tag{12} $$

Here, the summation can be substituted by the MI as:

$$ \sum_{i=0}^{Nos} (\Omega^{(2)}\Psi^{(2)}\Omega'^{(2)}S_3) = \frac{1}{1 - \Omega^{(2)}\Psi^{(2)}\Omega'^{(2)}S_3}. \tag{13} $$

Similarly, the scattering matrixes of the L-spheres system can deduced as:

$$ [{}^LT_1, {}^LT_2, {}^LT_3 \ldots {}^LT_L] = [G_1, G_2, G_3 \ldots G_L]\Psi^{(L)}, \tag{14} $$

where

$$ \Psi_{LL}^{(L)} = S_L \sum_{i=0}^{Nos} (\Omega^{(L-1)}\Psi^{(L-1)}\Omega'^{(L-1)}S_L)^i, $$

$$ \Psi_{pL}^{(L)} = \sum_{j=1}^{L-1} \Psi_{pj}^{(L-1)}\Omega_{j,L}\Psi_{LL}^{(L)} \quad p = 1 \ldots L-1, $$

$$ \Psi_{Lq}^{(L)} = \Psi_{LL}^{(L)} \sum_{j=1}^{L-1} \Omega_{L,j}\Psi_{jq}^{(L-1)} \quad q = 1 \ldots L-1, $$

$$\Psi_{pq}^{(L)} = \Psi_{pq}^{(L-1)} + \Psi_{pL}^{(L)} \sum_{j=1}^{L-1} \Omega_{L,j} \Psi_{jq}^{(L-1)} \quad p,q = 1 \ldots L-1,$$

where $\Omega^{(L-1)} = [\Omega_{L1}, \Omega_{L2}, ..., \Omega_{L,L-1}]$ and $\Omega'^{(L-1)} = [\Omega_{L1}, \Omega_{L2}, ..., \Omega_{L,L-1}]^{\mathrm{T}}$. The summation of the different orders of scattering matrix can be obtained by the MI as

$$\sum_{i=0}^{Nos} (\Omega^{(L-1)} \Psi^{(L-1)} \Omega'^{(L-1)} S_L) = \frac{1}{1 - \Omega^{(L-1)} \Psi^{(L-1)} \Omega'^{(L-1)} S_L}. \tag{15}$$

In this approach, we start from single sphere, two spheres, three spheres and recursively to obtain the scattering matrix of L spheres. We draw attention to the fact that the dimension of the matrix of a L-spheres system for inversion in Eq. (15) is of same size as that of a single sphere, which can greatly deduce the simulation time.

3. Electromagnetic energy transport in metal nanoparticle chains

How to transport light energy in metal nanoparticle chains below the diffraction limit is a fundamental problem of integrated optics [4,31]. The transport procedure involves the near-field coupling between surface plasmon–polariton modes of adjacent nanoparticles [2]. Here we investigate the 3 dB damping length of a chain of equal spacing Ag nanospheres with radius $R = 25$ nm, in which only the first Ag sphere is irradiated by incident light. The 3 dB damping length is defined as the intensity of light decreasing to the $10^{-0.3}$ of incident light. The investigated field point is at the surface of the spheres shown in the inset of Fig. 1 marked with black points, and the number of Ag spheres L is set to large enough in order to overcome the influence of the back scattering from the end of the chain. Fig. 1 shows 3 dB damping length of the Ag chain at different frequency of the incident light, which polarization is parallel to the axis of the chain. The curves are corresponding to the 3 dB damping length vs. the frequency at different geometries of chains, where the gap between two nearest spheres surfaces are 2, 7.5, 25, and 50 nm, respectively. Unlike the investigations of the light propagation at a fixed frequency in Ref. [4], we found that there is a favorite coupling frequency corresponding to the largest 3 dB damping length at certain geometry of a chain. As the width of the gap decreases, the width of the resonance peak is broadening and the best coupling frequency is red shift due to the strong plasmon coupling between close-packed metal nanoparticles.

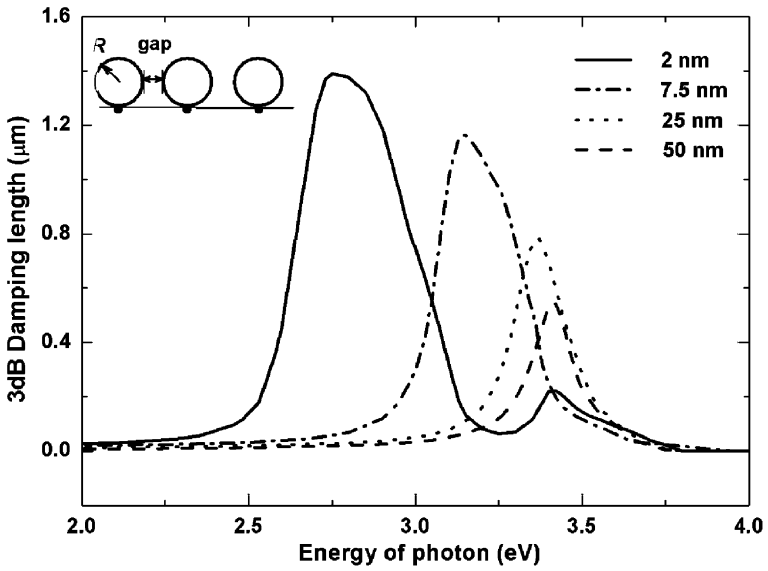

Fig. 1. The 3dB damping length vs. the energy of incident photon. The widths of the gap between neighboring spheres ($R = 25$ nm) are 2, 7.5, 25, and 50 nm, respectively. The investigated field points are marked with black points shown in the inset.

It should be noted that the simulation results are obtained using the method described above. The curves are smooth even at resonance condition. However, if we adopt the origin OS method, these curves become discrete close to the resonance frequency due to the no convergence of the summation of scattering orders at the resonance conditions. At the non-resonant frequency, these two methods give the same results which indicate both methods are correct in principle.

Fig. 2 shows the damping length varies with the gap between spheres at different incident frequencies. At certain frequency, there is an optimal guiding geometry, which is consistent with the conclusion obtained by Quinten et al. When the photon energy is larger than the plasmon resonance energy, the light can hardly transport via the Ag linear chains. For this case, the result of $E = 3.60\,\text{eV}$ is shown as the dashed line in Fig. 2. While at the plasmon resonance frequency of Ag nanoparticles at $E = 3.38\,\text{eV}$, the light can propagate a

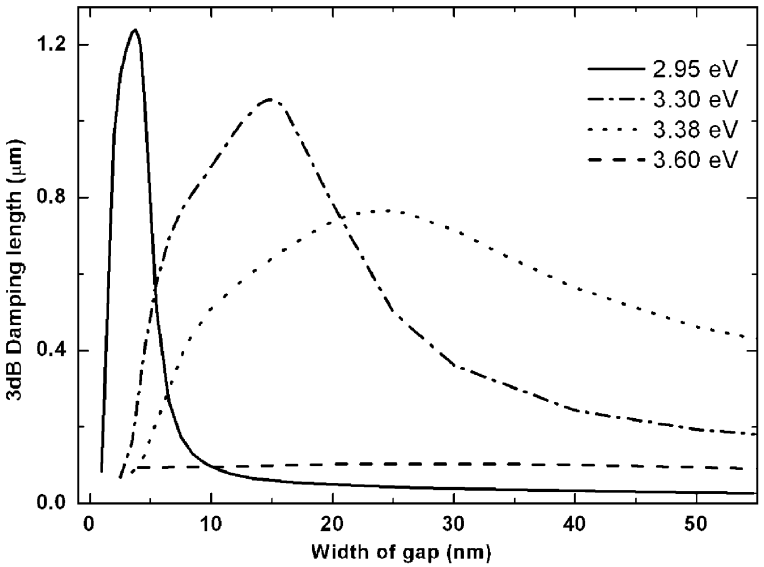

Fig. 2. The 3dB damping length vs. the width of gap between spheres at different photon energy 2.95, 3.30, 3.38, and 3.60 eV, respectively.

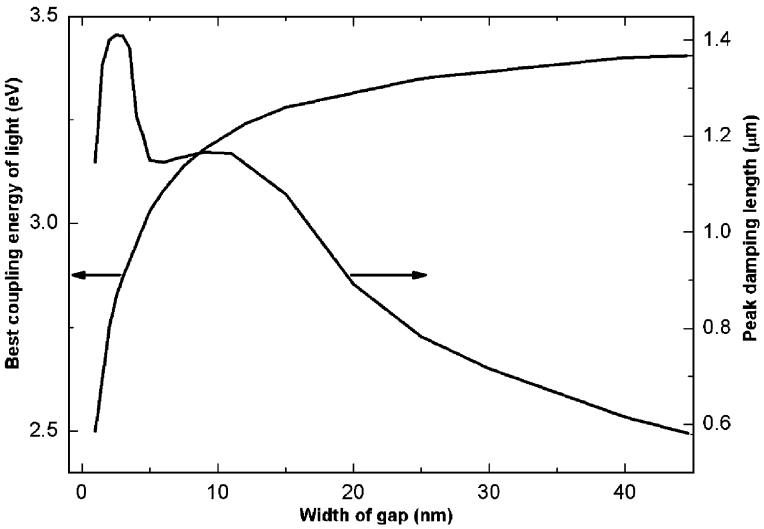

Fig. 3. Maximum 3dB damping length (to the right) and the corresponding favorite incident photon energy (to the left) vs. the width of gap between neighboring spheres.

considerable distance even for large gaps between nanoparticles as shown in the dotted line. The larger damping length is obtained at a lower incident frequency, e.g. $E = 2.95$ eV (solid line in Fig. 1), but a smaller gap is required and the band width becomes very narrow as well.

Fig. 3 shows the maximum 3 dB damping length of the light that transports via linear Ag chains with a fixed radius of sphere 25 nm at different separation between two adjacent spheres (to the right). For a small gap of a 3 nm gap, the maximum 3 dB damping length is ~1.36 μm, and the corresponding incident photon energy is about 2.88 eV. At the small-gap region, the propagation of the light is strongly dependent on the size of the gap, which indicates a strong geometric resonance based on the resonant plasmon coupling among metal nanoparticles. However, when the gap becomes more than 5 nm, the propagation of the light is not so sensitive to the size of the gap, and the maximum damping length slowly decrease with the increase of the size of the gap. At the "large-gap" region, the plasmon coupling between metal nanoparticles becomes weak with the increase of the size of the gap, while the single-particle plasmon resonance becomes the driving force to promote the propagation of the light. For a 3 dB damping length >0.6 μm, the energy of photon that transports via linear Ag chains investigated here has to be in the range from 2.5 to 3.42 eV (362–495 nm).

4. Summary

Here we develop a MI approach based on the recursive OS method to calculate the optical near-field of aggregates of nanospheres. By introducing the MI technique, the divergent problem encountered in the origin OS method is avoided. Moreover, the dimension of matrix in this method does not increase with the number of spheres L, which largely speed up the calculations than the T-matrix method where the dimension of the matrix increases as L^2. With this new method, we investigate the light-transport properties of Ag chains of nanospheres. We found that the damping lengths of linear chains of Ag spheres with a fixed radius $R = 25$ nm were dependent on both the incident frequency and the width of the gap between neighboring spheres. For a fixed width of the gap, there exists a best coupling frequency, and vice versa. The maximal 3 dB damping length can reach 1.4 μm for a proper geometry and incident frequency.

Acknowledgment

We thank Ke Zhao for the useful discussion. Xu acknowledges the financial support from the "100 Persons Project" of the Chinese Academy of Sciences.

References

[1] Xu HX. Electromagnetic energy flow near nanoparticles—I: single spheres. J Quant Spectrosc Radiat Transfer 2004;87:53–67.
[2] Maier SA, Kik PG, Atwater HA, Meltzer S, Harel E, Koel BE, et al. Local detection of electromagnetic energy transport below the diffraction limit in metal nanoparticle plasmon waveguides. Nat Mater 2003;2:229–32.
[3] Xu HX, Käll M. Surface-plasmon-enhanced optical forces in silver nanoaggregates. Phys Rev Lett 2002;89:246802.
[4] Quinten M, Leitner A, Krenn JR, Aussenegg FR. Electromagnetic energy transport via linear chains of silver nanoparticles. Opt Lett 1998;23:1331–3.
[5] Mishchenko MI, Travis LD, Mackowski DW. T-matrix computations of light scattering by nonspherical particles: a review. J Quant Radiat Transfer 1996;55:535–75.
[6] Xu HX. A new method by extending Mie theory to calculate local field in outside/inside of aggregates of arbitrary spheres. Phys Lett A 2003;312:411–9.
[7] Fuller KA. Optical resonances and two-sphere systems. Appl Opt 1991;30:4716–31.
[8] Mie G. Beitrage zur optik truber medien seziell kolloidaler matallösungen. Ann Phys 1908;25:377–455.
[9] Peterson B, Ström S. T Matrix for electromagnetic scattering from an arbitrary number of scatterers and representations of E(3)*. Phys Rev D 1973;8:3361–678.
[10] Mackowski DW, Mishchenko MI. Calculation of the T matrix and the scattering matrix for ensembles of spheres. J Opt Soc Am A 1996;13:2266–78.
[11] García de Abajo FJ. Multiple scattering of radiation in clusters of dielectrics. Phys Rev B 1999;60:6086–102.
[12] García de Abajo FJ. Interaction of radiation and fast electrons with clusters of dielectrics a multiple scattering approach. Phys Rev Lett 1999;82:2776–9.
[13] García de Abajo FJ. Smith-Purcell radiation emission in aligned nanoparticles. Phys Rev E 2000;61:5743–52.

[14] Stefanou N, Yannopapas V, Modinos A. Multem 2: a new version of the program for transmission and band-structure calculations of photonic crystals. Comput Phys Commun 2000;132:189–96.
[15] Stefanou N, Yannopapas V, Modinos A. Heterostructures of photonic crystals: frequency bands and transmission coefficients. Comput Phys Commun 1998;113:49–77.
[16] Käll M, Xu H, Johansson P. Field enhancement and molecular response in surface-enhanced Raman scattering and fluorescence spectroscopy. J Raman Spectrosc 2005;36:510–4.
[17] Xu HX, Aizpurua J, Käll M, Apell P. Electromagnetic contributions to single-molecule sensitivity in surface-enhanced Raman scattering. Phys Rev E 2000;62:4318–24.
[18] Flatau PJ, Fuller KA, Mackowski DW. Scattering by two spheres in contact: comparisons between discrete-dipole approximation and modal analysis. Appl Opt 1993;32:3302–5.
[19] Videen G, Sun W, Fu Q. Light scattering from irregular tetrahedral aggregates. Opt Commun 1998;156:5–9.
[20] Chew WC, Jin JM, Lu CC. Fast solution methods in electromagnetics. IEEE Trans Antennas Propag 1997;45:533–43.
[21] Comberg U, Wriedt T. Comparison of scattering calculations for aggregated particles based on different models. J Quant Spectrosc Radiat Transfer 1999;63:149–62.
[22] Waterman PC. Symmetry, unitarity, and geometry in electromagnetic scattering. Phys Rev D 1971;3:825–39.
[23] Bruning JH, Lo YT. Multiple scattering of EM waves by spheres. I. Multipole expansion and ray-optical solutions. IEEE Trans Antennas Propag 1971;AP-19:378–90.
[24] Hamid AK, Ciric IR, Hamid M. Iterative solution of the scattering by an arbitrary configuration of conducting or dielectric spheres. IEE Proc H 1991;138:565–72.
[25] Wang YM, Chew WC. A recursive T-matrix approach for the solution of electromagnetic scattering by many spheres. IEEE Trans Antennas Propag 1993;41:1633–9.
[26] Xu HX. Calculation of the near field of aggregates of arbitrary spheres. J Opt Soc Am 2004;21:804–9.
[27] Fuller KA, Kattawar GW. Consummate solution to the problem of classical electromagnetic scattering by an ensemble of spheres. I: Linear chains. Opt Lett 1988;18:90–2.
[28] Stratton JA. Electromagnetic theory. New York: McGraw-Hill; 1941.
[29] Stein S. Addition theorems for spherical wave functions. Q Appl Math 1961;19:15–24.
[30] Cruzan OR. Translational additional theorems for spherical vector wave functions. Q Appl Math 1962;20:33–40.
[31] Maier SA, Kik PG, Atwater HA. Optical pulse propagation in metal nanoparticle chain waveguides. Phys Rev B 2003;67:205402.